

UC Santa Barbara

UC Santa Barbara Previously Published Works

Title

Widely tunable bottom-emitting vertical-cavity SOAs

Permalink

<https://escholarship.org/uc/item/6f5653zs>

Journal

IEEE Photonics Technology Letters, 17(12)

ISSN

1041-1135

Authors

Cole, G D
Bjorlin, E S
Wang, C S
et al.

Publication Date

2005-12-01

Peer reviewed

Widely Tunable Bottom-Emitting Vertical-Cavity SOAs

Garrett D. Cole, *Student Member, IEEE*, E. Staffan Björilin, *Member, IEEE*, Chad S. Wang, *Student Member, IEEE*, Noel C. MacDonald, *Fellow, IEEE*, and John E. Bowers, *Fellow, IEEE*

Abstract—We present bottom-emitting tunable vertical-cavity semiconductor optical amplifiers (VC SOAs) with an effective wavelength tuning range of >20 nm. These devices utilize a high reflectivity micromechanically tunable Bragg mirror as the back reflector. Compared with our first generation tunable VC SOAs, the bottom-emitting devices exhibit a two-fold increase in the effective tuning range as well as a five-fold reduction in the required tuning voltage.

Index Terms—Fabry–Pérot resonators, laser amplifiers, microelectromechanical (MEMS) devices, semiconductor optical amplifiers, surface-emitting lasers, tunable amplifiers, wafer bonding.

I. INTRODUCTION

VERTICAL-CAVITY semiconductor optical amplifiers (VC SOAs) have numerous potential applications in fiber-optic communication systems including use as preamplifiers, optical switches, and modulators [1]. In these applications, the vertical-cavity geometry gives rise to a number of advantages including a high fiber-coupling efficiency, polarization-independent gain, decreased power consumption, the potential to fabricate two-dimensional (2-D) arrays, and the ability to test on wafer.

As small form-factor 2-D arrays, VC SOAs are a low-cost alternative to existing amplifier technologies. The inherent filtering effect of the high-finesse Fabry–Pérot cavity eliminates the need for an optical filter after the amplifier making VC SOAs ideal as preamplifiers in high bit-rate receivers [2]. For reconfigurable optical networks, it is of interest to develop widely tunable VC SOAs that can be precisely adjusted to match the wavelength of the desired input signal. Moreover, because VC SOAs operate as amplifying filters, the addition of tunability allows for the creation of wavelength agile filters with the added benefit of optical gain.

As an extension of fixed-wavelength devices, we have developed widely tunable VC SOAs through the incorporation of an integrated microelectromechanical (MEMS) actuator [3], [4]. In contrast with temperature tuning [1], [5], the AlGaAs-based electrostatic actuator used in our MEMS-tunable

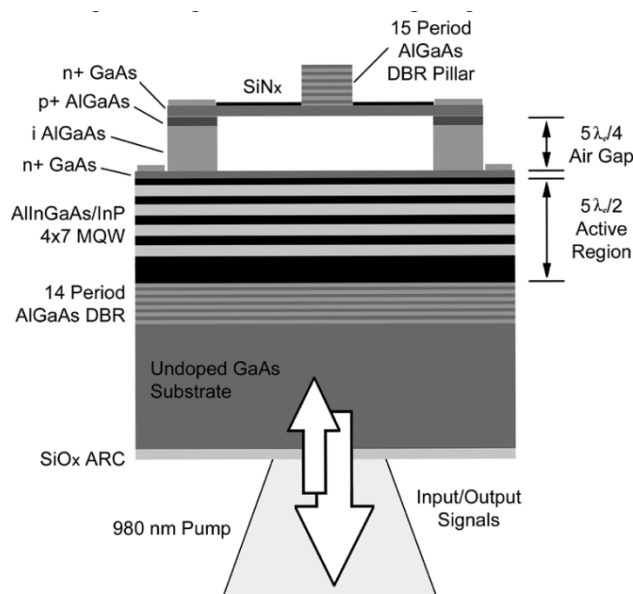


Fig. 1. Cross-sectional schematic of the bottom-emitting tunable VC SOA.

VC SOAs (MT-VC SOAs) allows for rapid, low power, and wide wavelength tuning [6]. However, in our first generation of top-emitting devices, the use of the MEMS structure as the transmissive mirror resulted in a large variation in reflectance with tuning, limiting the effective tuning range [3], [4].

Here, we report new bottom-emitting reflection-mode MT-VC SOAs in which the optical cavity is inverted and the MEMS-tuning structure serves as the high-reflectivity back mirror. By suppressing the variation in mirror reflectance, this configuration exhibits a two-fold increase in the effective tuning range—with a minimum of 5-dB fiber-to-fiber gain (12-dB on-chip gain) over a wavelength span of 21 nm, from 1557.4 to 1536.4 nm. Additionally, we record saturation, bandwidth, and noise properties similar to state-of-the-art fixed-wavelength VC SOAs. Through improvements to the electrostatic actuator, the maximum required tuning voltage has been reduced to 10.5 V, a five-fold reduction compared with the first generation of MT-VC SOAs [3].

II. DEVICE DESIGN AND FABRICATION

Fig. 1 shows a schematic of our bottom-emitting MT-VC SOAs. The devices are designed for optical pumping and operate in reflection mode, utilizing an InP-based active region wafer-bonded to two GaAs–AlGaAs distributed Bragg reflectors (DBRs). The stacked multiquantum-well active structure contains four sets of seven 0.85% compressively strained AlIn-

Manuscript received June 14, 2005; revised July 15, 2005. This work was supported in part by the National Science Foundation (NSF) IGERT Advanced Optical Materials (AOM) Program, award DGE-9987618.

G. D. Cole was with the Materials Department, University of California Santa Barbara, Santa Barbara, CA 93106 USA. He is now with Aeriis Photonics, LLC, Ventura, CA 93003 USA (e-mail: gcole@aeriisphotonics.com).

E. S. Björilin, C. S. Wang, and J. E. Bowers are with the Electrical and Computer Engineering Department, University of California Santa Barbara, Santa Barbara, CA 93106 USA.

N. C. MacDonald is with the Materials Department, University of California Santa Barbara, Santa Barbara, CA 93106 USA.

Digital Object Identifier 10.1109/LPT.2005.859157

GaAs quantum wells placed at the top four peaks of the standing optical wave in a $5\lambda/2$ cavity. In this design, the last standing-wave peak overlaps with a 276-nm-thick InP heat spreading layer. The addition of the binary heat spreading layer is important as the active region incorporates absorbing -0.55% tensile strained AlInGaAs barriers. The PL peak is designed to be at 1540 nm at room temperature.

In these devices, the transmissive bottom DBR consists of 14 periods of GaAs–Al_{0.98}Ga_{0.02}As, with a theoretical power reflectance of approximately 0.94. To reduce stray reflections from the substrate to air interface, we use a $\lambda/4$ SiO_x antireflection coating (ARC) with a measured power reflectance of 0.014 within the wavelength span of the MT-VCISOA.

From the top down, the high reflectivity MEMS-tunable mirror structure consists of 15 periods of GaAs–Al_{0.92}Ga_{0.08}As, a $3\lambda/4$ n⁺ GaAs membrane layer, an approximately $5\lambda/4$ (optical thickness in air) Al_{0.85}Ga_{0.15}As sacrificial etch layer and a $\lambda/4$ n⁺ GaAs layer directly above the active region. Selective removal of the sacrificial AlGaAs layer forms the variable air gap, which acts as the first low index layer in the MEMS-tunable DBR and forms the semiconductor coupled cavity tuning structure [4]. The peak power reflectance of the top mirror is calculated to be 0.996, including the contribution of the air gap and the loss from the doped layers that make up the electrostatic actuator. For the patterned portions of this structure, we use a reduced Al content to improve the reliability of the devices. This is especially important for the nearly 2- μ m-thick sacrificial AlGaAs layer, where oxidation in ambient air will lead to cracking of the support material beneath the GaAs membrane.

The details of the electrostatic actuator design are covered in [4] and [6]. A reverse bias across the p⁺-i⁺-n⁺ diode creates a Coulomb force that displaces the membrane toward the substrate, reducing the air-gap thickness and blue-shifting the resonant cavity mode. With this actuator, it is only possible to blue shift the resonant wavelength.

The basic fabrication procedure for our MT-VCISOAs is found in [3], [4]. The major differences in the bottom-emitting devices include the addition of an evaporated SiO_x quarter-wave transformer as an ARC, a revised wet etch for the selective removal of the Al_{0.85}Ga_{0.15}As sacrificial layer, and a reduction of the actuator film stress.

III. EXPERIMENTAL TESTING AND RESULTS

Fig. 2 shows a schematic of the optical test setup used for our bottom-emitting MT-VCISOAs. An external cavity tunable laser diode is used as the signal source and the input signal power is controlled by a variable optical attenuator to be -35 dBm. After combining with a wavelength-division-multiplexing (WDM) coupler, both the 980-nm pump and long-wavelength signal are coupled through the bottom of the sample with a single 1550-nm fiber focuser. As seen in the inset of Fig. 2, due to the wavelength-dependent focal length of the lens, there is a narrow range of stage positions where the pump spot size is slightly larger than that of the signal—the highlighted region is the approximate position used for testing. As the device operates in reflection, the amplified output returns through the same fiber focuser and is separated from the input signal using a circulator. All measurements are made with the output signal

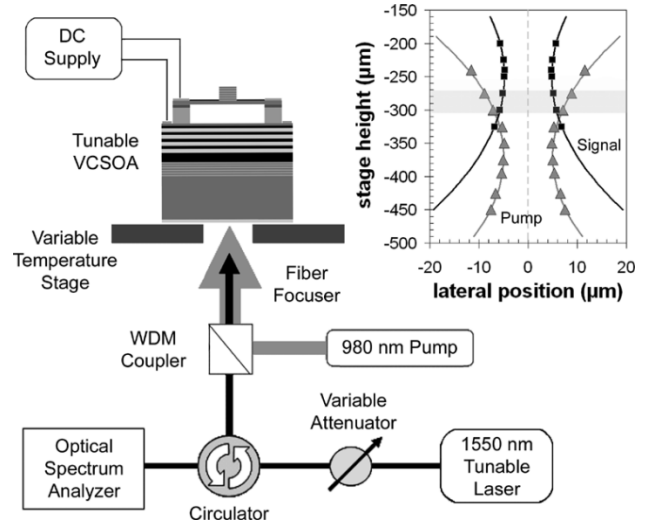


Fig. 2. Experimental setup used for the bottom-emitting MT-VCISOAs.

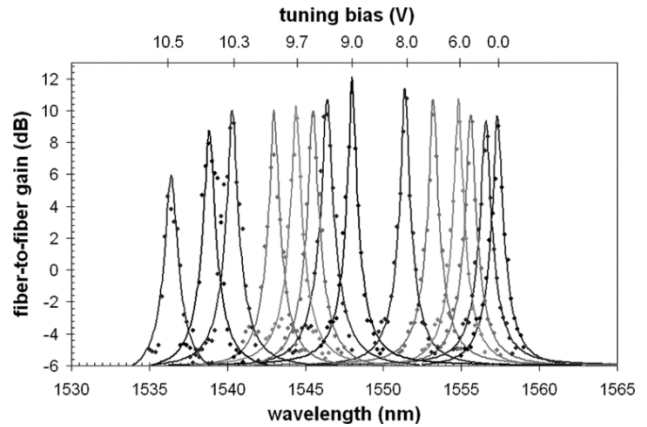


Fig. 3. Gain spectra over a >20 -nm wavelength range at 15°C for a constant pump power of 83 mW and a maximum tuning bias of 10.5 V.

coupled into single-mode fiber on a calibrated optical spectrum analyzer at a resolution bandwidth of 0.1 nm. The coupling loss through the setup is measured to be approximately 7 dB, including back-coupling of the output into the focuser (5.8 dB) and the round-trip through the WDM coupler and circulator (1.2 dB).

Fig. 3 presents the gain spectra of a bottom-emitting MT-VCISOA for an optical pump power of 83 mW and a stage temperature of 15°C . As seen in Fig. 3, the device is capable of at least 5-dB fiber-to-fiber gain (12-dB on-chip gain) over a 21-nm wavelength span, with a maximum applied voltage of 10.5 V. We record a peak fiber-to-fiber gain value of 11.2 dB (18.2-dB on-chip gain) at 1548.0 nm. Investigations of the peak gain as a function of pump power reveal that 83 mW is the optimal pump level for these devices. Note that with increased pump power, the device could not be brought to lasing threshold.

By fitting the individual gain spectra with the standard relationship for a reflection-mode Fabry–Pérot amplifier, we can extract the mirror reflectance values as well as the single-pass gain as a function of the resonant wavelength of the VCISOA [4]. From theoretical fitting of the gain spectra, we find that

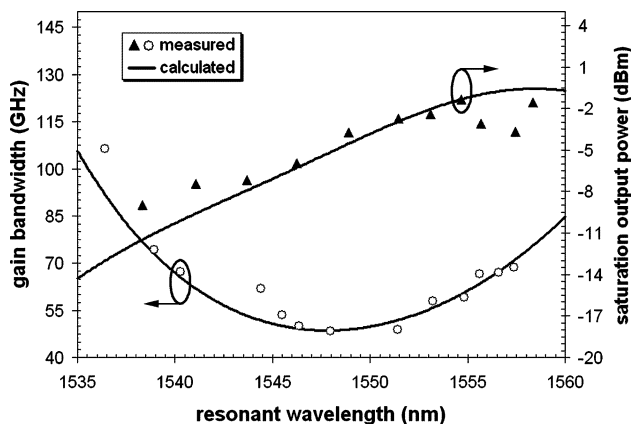


Fig. 4. Saturation output power and gain bandwidth as a function of resonant wavelength at 15 °C for a pump power of 83 mW.

the average single-pass gain is 3.5% over the tuning range at 83 mW. Combining this with the extracted mirror reflectance, the device is operating at an average of 97.8% of the single-pass gain required to reach threshold. In these devices, the peak gain appears to be limited by device self heating. With decreasing temperature the gain continually increases, however, low-temperature operation is limited by the ambient dew point. The pull-in instability of the electrostatic actuator is found to be the main failure mode and is also the limit of the overall wavelength tuning range.

Fig. 4 presents the saturation output power and gain bandwidth properties of our bottom-emitting MT-VC SOA. We measure a maximum fiber-coupled saturation output power of -1.4 dBm at 1554.7 nm, with an unsaturated fiber-to-fiber gain of 9.2 dB (16.2-dB on-chip gain). This value is comparable to the record high saturation output power of 0.5 dBm measured for our fixed wavelength devices [7] and is attributed to the low reflectivity of the transmissive mirror and the relatively large spot sizes used in the test setup. From Fig. 4, the average gain bandwidth of the device is 65.2 GHz over the 21-nm tuning range. Optical measurements of the amplifier noise [1] reveal a fiber-coupled noise figure of 7.5 dB for an average fiber-to-fiber gain of 9.0 dB. These properties are similar to state-of-the-art fixed-wavelength VC SOAs, confirming that the tuning mechanism does not sacrifice overall device performance. The calculated curves are based on the theoretical models in [4].

Previously, the best peak gain performance measured for our MT-VC SOAs was at least 3-dB fiber-to-fiber gain (10-dB on-chip gain) over 11 nm using a top emitting configuration with a transmissive tunable DBR [3]. These devices required large variations in pump power to maintain a constant signal gain, due to the significant variation in reflectance ($>10\%$) with tuning—arising from the destructive interference of the multiple reflections within the passive air cavity [3]. By inverting the optical cavity and using the MEMS-tuning structure as the high reflectivity mirror, we see a significant increase in the width of the peak gain envelope, as in Fig. 5, due to the more constant mirror properties with tuning, as predicted in [4]. For the bottom-emitting devices, the tunable mirror reflectance varies from a maximum value of 0.993 to a minimum of 0.986, a difference of only 0.7%.

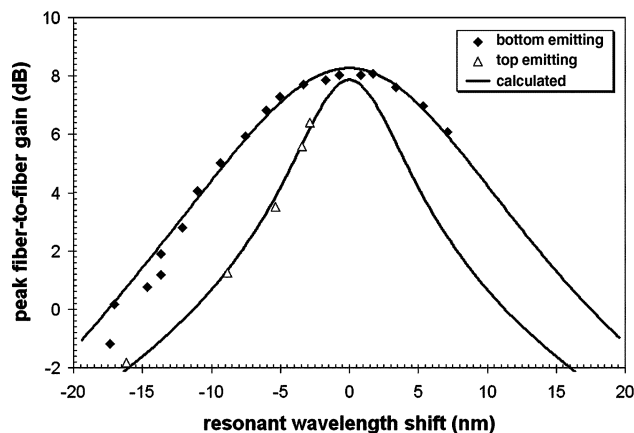


Fig. 5. Comparison of peak fiber-to-fiber gain at a constant pump power for two generations of MT-VC SOAs. Here we define the wavelength of peak gain as the center wavelength of the optical cavity.

IV. CONCLUSION

We present bottom-emitting MT-VC SOAs with inherently superior properties when compared with top-emitting devices utilizing a transmissive tunable mirror. The bottom-emitting devices incorporate a high reflectivity tunable DBR in order to suppress the variation in mirror reflectance with tuning. This configuration exhibits a minimum of 5 dB of fiber-to-fiber gain (12-dB on-chip gain) over 21 nm of tuning, with a constant pump power of 83 mW. Furthermore, we record a peak fiber-to-fiber gain of 11.2 dB (18.2-dB on-chip gain), a maximum saturation output power of -1.4 dBm, and an average gain bandwidth and noise figure of 65.2 GHz and 7.5 dB over the wavelength span, comparable to the current state of the art in fixed-wavelength VC SOAs—with the added flexibility of wide wavelength tuning.

REFERENCES

- [1] E. S. Björlin, T. Kimura, and J. E. Bowers, "Carrier-confined vertical-cavity semiconductor optical amplifiers for higher gain and efficiency," *IEEE J. Sel. Topics Quantum Electron.*, vol. 9, no. 9, pp. 1374–1385, Sep. 2003.
- [2] T. Kimura, E. S. Björlin, H.-F. Chou, Q. Chen, S. Wu, and J. E. Bowers, "Optically preamplified receiver at 10, 20, and 40 Gb/s using a 1550-nm vertical-cavity SOA," *IEEE Photon. Technol. Lett.*, vol. 17, no. 2, pp. 456–458, Feb. 2005.
- [3] Q. Chen, G. D. Cole, E. S. Björlin, T. Kimura, S. Wu, C. S. Wang, N. C. MacDonald, and J. E. Bowers, "First demonstration of a MEMS-tunable vertical-cavity SOA," *IEEE Photon. Technol. Lett.*, vol. 16, no. 6, pp. 1438–1440, Jun. 2004.
- [4] G. D. Cole, E. S. Björlin, Q. Chen, C.-Y. Chan, S. Wu, C. S. Wang, N. C. MacDonald, and J. E. Bowers, "MEMS-tunable vertical-cavity SOAs," *IEEE J. Quantum Electron.*, vol. 41, no. 3, pp. 390–407, Mar. 2005.
- [5] A. H. Clark, S. Calvez, N. Laurand, R. Macaluso, H. D. Sun, M. D. Dawson, T. Jouhti, J. Kontinen, and M. Pessa, "Long-wavelength monolithic GaInNAs vertical-cavity optical amplifiers," *IEEE J. Quantum Electron.*, vol. 40, no. 7, pp. 878–883, Jul. 2004.
- [6] G. D. Cole, J. E. Bowers, K. L. Turner, and N. C. MacDonald, "Dynamic characterization of MEMS-tunable vertical-cavity SOAs," in *Tech. Proc. 2005 IEEE/LEOS Int. Conf. Optical MEMS and Their Applications*, Oulu, Finland, Aug. 1–4, 2005, Paper F4, pp. 99–100.
- [7] E. S. Björlin, T. Kimura, Q. Chen, C. Wang, and J. E. Bowers, "High output power 1540 nm vertical cavity semiconductor optical amplifiers," *Electron. Lett.*, vol. 40, pp. 121–123, Jan. 2004.